AMERICAN SOCIETY FOR MICROBIOLOGY | Journal of Virology®

VIRUS-CELL INTERACTIONS

Tight Junction Protein Occludin Is a Porcine Epidemic Diarrhea Virus Entry Factor

Xiaolei Luo, Longjun Guo, Jian Zhang, Yunfei Xu, Weihong Gu, Li Feng, Yue Wang

State Key Laboratory of Veterinary Biotechnology, Harbin Veterinary Research Institute, Chinese Academy of Agricultural Sciences, Harbin, China

ABSTRACT Porcine epidemic diarrhea virus (PEDV), the causative agent of porcine epidemic diarrhea, has caused huge economic losses in pig-producing countries. Although PEDV was long believed to replicate in the intestinal epithelium by using aminopeptidase N as a receptor, the mechanisms of PEDV infection are not fully characterized. In this study, we found that PEDV infection of epithelial cells results in disruption of the tight junctional distribution of occludin to its intracellular location. Overexpression of occludin in target cells makes them more susceptible to PEDV infection, whereas ablation of occludin expression by use of small interfering RNA (siRNA) in target cells significantly reduces their susceptibility to virus infection. However, the results observed with occludin siRNA indicate that occludin is not required for virus attachment. We conclude that occludin plays an essential role in PEDV infection at the postbinding stages. Furthermore, we observed that macropinocytosis inhibitors blocked occludin internalization and virus entry, indicating that virus entry and occludin internalization are closely coupled. However, the macropinocytosis inhibitors could not impede virus replication once the virus had entered host cells. This suggests that occludin internalization by macropinocytosis or a macropinocytosis-like process is involved in the virus entry events. Immunofluorescence confocal microscopy showed that PEDV was trapped at cellular junctional regions upon macropinocytosis inhibitor treatment, indicating that occludin may serve as a scaffold in the vicinity of virus entry. Collectively, these data show that occludin plays an essential role in PEDV infection during late entry events. Our observation may provide novel insights into PEDV infection and related pathogenesis.

IMPORTANCE Tight junctions are highly specialized membrane domains whose main function is to attach adjacent cells to each other, thereby forming intercellular seals. Here we investigate, for the first time, the role of the tight junction protein occludin in PEDV infection. We observed that PEDV infection induced the internalization of occludin. By using genetic modification methods, we demonstrate that occludin plays an essential role in PEDV infection. Moreover, PEDV entry and occludin internalization seem to be closely coupled. Our findings reveal a new mechanism of PEDV infection.

KEYWORDS PEDV, occludin, tight junction

Coronaviruses are a group of positive-strand RNA viruses belonging to the family *Coronaviridae* in the order *Nidovirales*. They are broadly distributed among mammalian and avian species, and they cause acute and persistent infections. In most cases, coronaviruses are generally associated with significant respiratory and/or intestinal tract diseases (1, 2). Porcine epidemic diarrhea virus (PEDV) has been identified as the etiologic agent of porcine epidemic diarrhea (PED), and it causes diarrhea, vomiting, and dehydration in infected swine (3, 4). Outbreaks of PED have occurred frequently in

Received 5 February 2017 **Accepted** 28 February 2017

Accepted manuscript posted online 8 March 2017

Citation Luo X, Guo L, Zhang J, Xu Y, Gu W, Feng L, Wang Y. 2017. Tight junction protein occludin is a porcine epidemic diarrhea virus entry factor. J Virol 91:e00202-17. https://doi.org/10.1128/JVI.00202-17.

Editor Stanley Perlman, University of Iowa

Address correspondence to Yue Wang, wangyue@hvri.ac.cn.

X.L. and L.G. contributed equally to this article.

many swine-raising countries in Europe, Asia, and America, resulting in considerable economic losses (5–10).

As noted earlier, epidemic PEDV strains are highly enteropathogenic and mainly infect villous epithelial cells of the small intestine before disseminating (11, 12). It is well known that the intestinal epithelium has two important functions: absorbing helpful substances and providing a physical fence against harmful substances. The essential components of this epithelial barrier are physical intercellular structures, termed tight junctions, which attach adjacent cells to each other, thereby forming intercellular seals (13, 14). Many proteins are specifically localized to tight junctions, including cytoplasmic actin-binding proteins and adhesive transmembrane proteins. Among them, the major types of proteins in junctions are the claudin and occludin proteins (15). Many pathogens that infect epithelial cells have evolved elaborate strategies to bypass this barrier and establish their infections. The precise mechanisms regulating PEDV entry into intestinal epithelial cells remain unknown, although porcine aminopeptidase N (APN) has been identified as a functional receptor for PEDV infection (16–18).

In recent years, increasing evidence has shown that some viruses can hijack the different components of tight junctions to initiate infections (for reviews, see references 19–22). For example, the tight junction protein occludin has been identified as an essential host factor for entry of several viruses, such as coxsackie B virus (CBV), rotavirus, human hepatitis C virus (HCV), West Nile virus, and others (21, 23–25). In addition to occludin, the tight junction protein claudin-1 is tightly related to the infection of dengue virus, HCV, West Nile virus, and others (25–28). During PEDV infection, it has been demonstrated that structural destruction and disorganization of tight junctions are observed (12, 29). However, the role of tight junctions in PEDV infection has not yet been defined. In the present study, we observed that the tight junction protein occludin disappeared from its normal location in PEDV-infected cells. By using genetic modification methods, we demonstrated that occludin plays an essential role in PEDV entry. Confocal microscopy data provided further evidence that macropinocytosis-mediated occludin internalization is involved in virus entry. These findings highlight an important role for occludin in mediating virus entry and subsequent replication.

RESULTS

PEDV infection alters the expression and distribution of occludin in target cells. PEDV causes an acute and devastating viral enteric disease. This virus enters its host through the fecal-oral route and must cross the intestinal mucosa in order to reach its target cells to initiate infection (12). To do so, this virus must gain access to the tight junctions. To understand the correlation between tight junctions and PEDV infection, we first analyzed the mRNA and protein levels of the tight junction proteins occludin and claudin-1 in virus-infected IPEC-J2 and Vero E6 cells. As determined by quantitative PCR, the mRNA levels for claudin-1 revealed no remarkable change following PEDV infection; however, the mRNA levels for occludin were significantly upregulated in PEDV-infected IPEC-J2 and Vero E6 cells at 24 and 48 h postinfection (hpi) (Fig. 1A and 2A). Similarly, the protein levels of occludin were increased in virus-infected IPEC-J2 and Vero E6 cells at 24 and 48 hpi, whereas the protein levels of claudin-1 had changed little during the course of PEDV infection (Fig. 1B and 2B).

To further understand the relationship between tight junctions and PEDV infection, we examined the cellular distribution of occludin and claudin-1 in IPEC-J2 cells upon virus infection. The immunofluorescence microscopy results showed that the tight junction protein occludin showed a pronounced distribution at the cell-cell junction in mock-treated IPEC-J2 cells; however, in PEDV-infected cells, occludin staining was less evident in the junctional area, and there was an increased cytoplasmic distribution of this protein (Fig. 1C). In contrast, PEDV infection did not markedly alter the cell junctional localization of the tight junction protein claudin-1 (Fig. 1D). To ensure that these observations were not limited to the specific cell type used, we repeated these experiments with Vero E6 cells. Consistent with the findings obtained with IPEC-J2 cells,

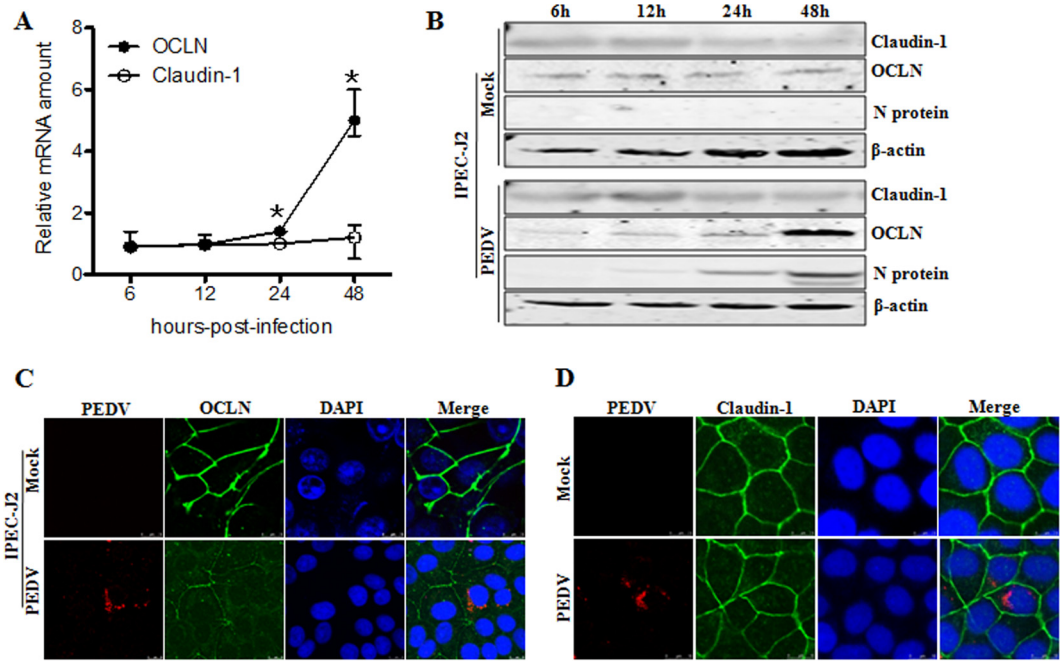

FIG 1 PEDV infection alters occludin (OCLN) expression and distribution in IPEC-J2 cells. (A) PEDV infection leads to upregulation of occludin mRNA. IPEC-J2 cells were infected with PEDV at an MOI of 1. At 6, 12, 24, and 48 hpi, RNA was extracted and quantitative PCR analysis performed as described in Materials and Methods. (B) Expression levels of occludin are increased in IPEC-J2 cells upon PEDV infection. Cell monolayers were infected with PEDV at an MOI of 1 and further cultured as indicated. Cell lysates were subjected to immunoblotting with antibodies to occludin, claudin-1, PEDV nucleocapsid protein, or β-actin (loading control). (C and D) PEDV infection alters the distribution of occludin but not that of claudin-1. IPEC-J2 cells were infected with PEDV at an MOI of 1 and cultured for another 24 h. Cells were fixed, and triple-color immunofluorescence staining and confocal microscopy were used to detect and analyze the virus (red), occludin/claudin-1 (green), and the nucleus (blue), using a Leica SP2 confocal laser scanning microscope. Results are representative of three independent experiments (means $\pm$ SD). *, $P < 0.05$. The P value was calculated using Student's t test.

the cellular distribution of occludin shifted from mostly junctional localization to a punctate cytoplasmic signal in PEDV-infected Vero E6 cells, while claudin-1 remained at the typical cell-cell junctional region during PEDV infection (Fig. 2C and D). These data indicate that PEDV infection induces the internalization of the tight junction protein occludin, but not claudin-1, in target cells, suggesting that alteration of occludin protein distribution may contribute to PEDV infection.

Overexpression of occludin facilitates PEDV infection. To characterize the role of occludin in PEDV infection, we surveyed the relationship between its expression and virus susceptibility in a variety of cell lines. First, we tested whether overexpression of occludin in Vero E6 and IPEC-J2 cells would increase their susceptibility to PEDV infection. These cells were transduced with a bicistronic lentiviral vector expressing porcine occludin and ZsGreen (green fluorescent protein), which is expressed in a proportional manner. A lentivirus encoding ZsGreen only served as a vector control. As shown in Fig. 3A, more than 95% of Vero E6 and IPEC-J2 cells were green fluorescence positive, indicating that the lentiviruses were successfully transduced into cells. The Western blot results confirmed that occludin was overexpressed in both types of cells (Fig. 3B). PEDV infectivity in occludin-overexpressing Vero E6 and IPEC-J2 cells increased 4.1- and 11.5-fold, respectively, compared to that in vector control-treated parental cells (Fig. 3C). We next examined the effect of occludin overexpression on the PEDV yield by measuring the 50% tissue culture infective dose ($TCID_{50}$). The data showed that viral yields were higher in occludin-overexpressing Vero E6 cells (6.4 ± 0.3 $\log_{10}$ $TCID_{50}$/ml) and IPEC-J2 cells (3.8 ± 0.3 $\log_{10}$ $TCID_{50}$/ml) than in vector control-treated Vero E6 cells (5.5 ± 0.4 $\log_{10}$ $TCID_{50}$/ml) and IPEC-J2 cells (2.9 ± 0.4 $\log_{10}$ $TCID_{50}$/ml), respectively (Fig. 3D). However, the PEDV-resistant cell line BHK also expressed detectable levels of endogenous occludin and remained PEDV resistant when it overex-

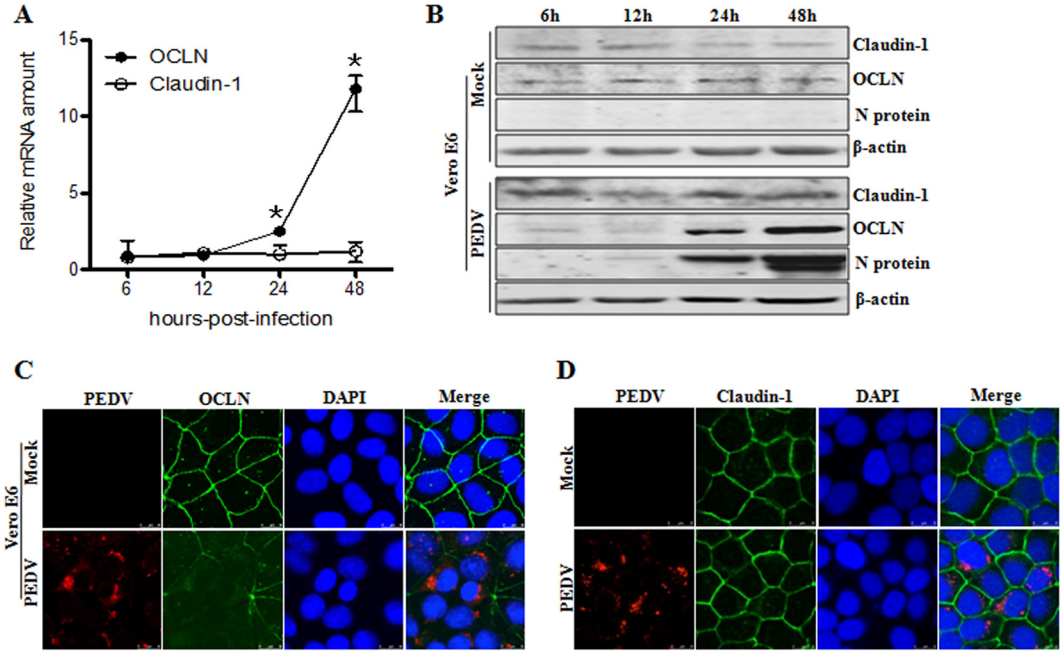

FIG 2 PEDV induces occludin internalization in virus-infected Vero E6 cells. (A) Quantitative PCR assay to detect the levels of occludin and claudin-1 in PEDV-infected Vero E6 cells. Cells were mock infected or infected with PEDV at an MOI of 0.1 and cultured for the indicated times. Total RNA was used to determine the mRNA levels of occludin and claudin-1 by quantitative PCR assay. (B) Protein levels of occludin and claudin-1 in PEDV-infected Vero E6 cells. Cells were infected with PEDV at an MOI of 0.1. Cell lysates were collected at 6, 12, 24, and 48 hpi and subjected to immunoblotting with the indicated antibodies. PEDV infection caused the internalization of occludin (C), but not claudin-1 (D), in Vero E6 cells. Vero E6 cells were mock infected or infected with PEDV at an MOI of 0.1. At 24 hpi, the cell monolayer was stained for the virus (red), occludin/claudin-1 (green), and the nucleus (blue). Results are representative of three independent experiments (means ± SD). *, $P < 0.05$. The *P* value was calculated using Student's *t* test.

pressed occludin (data not shown). These observations demonstrate that the presence of occludin renders target cells more susceptible to PEDV infection, although directed expression of occludin alone is not sufficient to render cells susceptible, suggesting that occludin plays an important role in virus infection.

Knockdown of endogenous occludin expression inhibits PEDV infection. To determine whether the tight junction protein occludin is required for efficient PEDV infection of permissive cells, IPEC-J2 cells were transfected with small interfering RNA (siRNA) duplexes targeting the *occludin* gene. The expression of the occludin protein was determined by Western blotting and immunofluorescence assay. As shown in Fig. 4A, cells transfected with occludin-specific siRNA showed a marked reduction in the level of occludin protein. Additionally, immunofluorescence data showed that the cell-cell junctional distribution of occludin protein was dramatically decreased in occludin siRNA-transfected cells (Fig. 4B). In contrast, we did not note any evident changes in the expression and staining pattern of claudin-1 in occludin siRNA-transfected cells compared to those in control siRNA-treated cells (Fig. 4A and B), suggesting that *occludin* gene silencing does not impair the integrity of tight junctions in target cells. Using these cells, we investigated the influence of occludin on PEDV entry and replication. As shown in Fig. 4C, the susceptibility of occludin-silenced IPEC-J2 cells to PEDV infection was approximately 70% lower than that of control cells as determined by enumeration of PEDV-positive cells following immunofluorescence labeling. The reduction in the titer of progeny virus in occludin knockdown cells was confirmed by measuring the $TCID_{50}$ (Fig. 4D). As was the case with IPEC-J2 cells, silencing the endogenous expression of occludin in Vero E6 cells (Fig. 4E and F) decreased the efficiency of PEDV infection (Fig. 4G) and reduced viral yields compared to those in cells treated with control siRNA (Fig. 4H). Taken together, these data demonstrate that knockdown of endogenous occludin expression in target cells results in their reduced

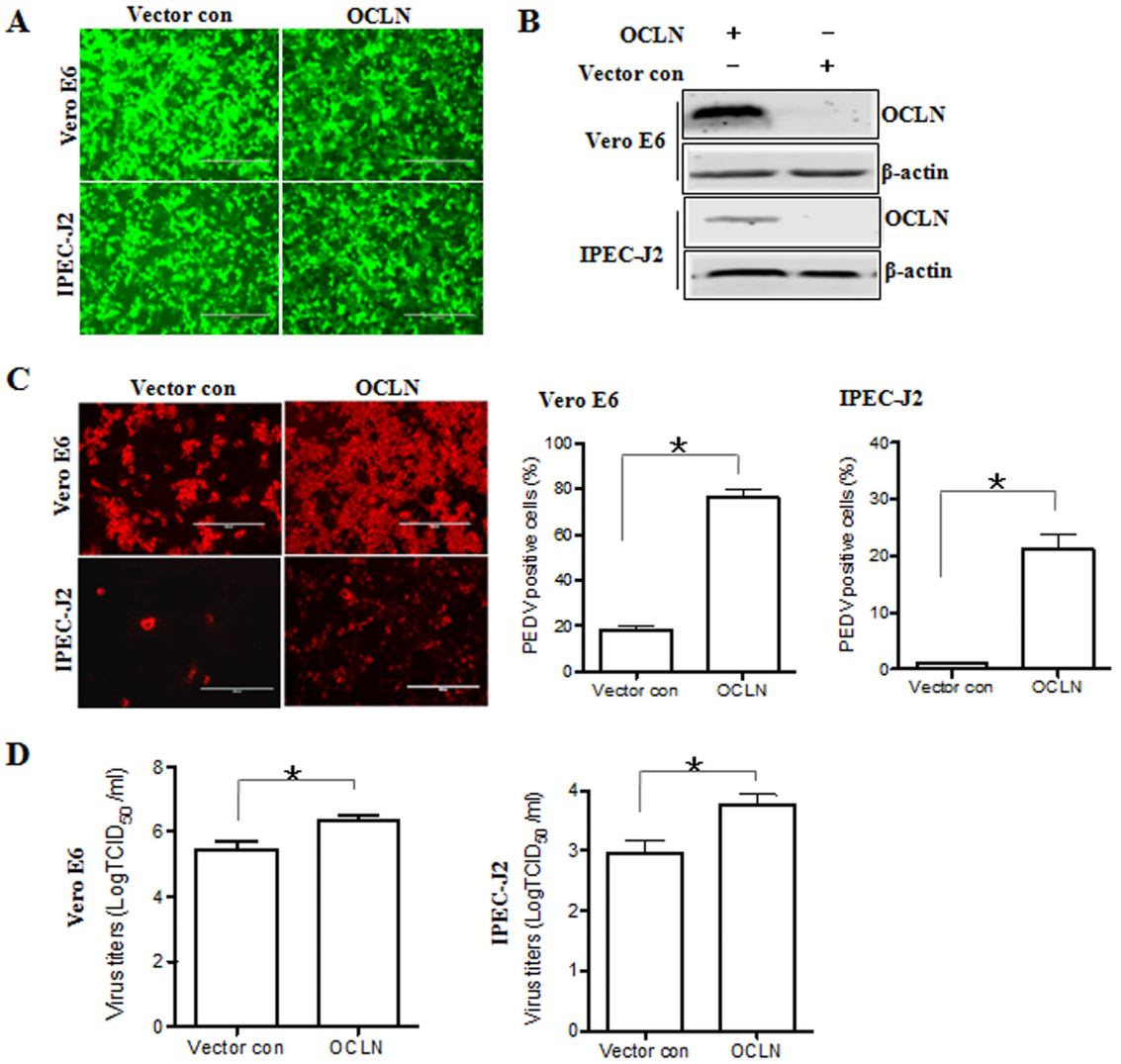

FIG 3 Overexpression of occludin facilitates PEDV infection. (A) Vero E6 and IPEC-J2 cells were transduced with a bicistronic lentivirus vector expressing ZsGreen alone (vector control) or occludin plus ZsGreen as described in Materials and Methods. (B) Overexpression of occludin in Vero E6 and IPEC-J2 cells. Detergent lysates from cells transduced with occludin or the vector control were subjected to immunoblotting with the indicated antibodies. (C) Occludin overexpression enhances PEDV infection as detected by immunofluorescence assay. Vero E6 and IPEC-J2 cells were transduced with the vector control or occludin as described above and then infected with PEDV at MOIs of 0.1 and 1, respectively, for 24 h. The percentage of PEDV-infected cells was determined by immunofluorescence staining with anti-PEDV spike protein MAb. (D) Occludin overexpression enhances PEDV replication as determined by $TCID_{50}$ assay. The cell monolayer was exposed to PEDV 24 h after transduction with occludin or the vector control. At 48 hpi, virus yields were determined by $TCID_{50}$ assay with Vero E6 cells. Results are representative of three independent experiments (means ± SD). *, $P < 0.05$. The *P* value was calculated using Student's *t* test.

susceptibility to PEDV infection, suggesting that the tight junction protein occludin is essential for PEDV infection.

Occludin knockdown does not affect initial PEDV attachment. Coronavirus infection is initiated by the binding of viral particles to specific proteins on the cell surface (26). We carried out PEDV virion binding assays in order to determine whether the occludin protein plays an essential role in initial virus binding events. Vero E6 cells were first transfected with control siRNA or occludin-specific siRNA to knock down the expression of endogenous occludin. At 24 h posttransfection, cells were incubated with PEDV for 2 h at 4°C so that virion binding, but not entry, could occur. After removal of excess virions, total RNA was extracted to determine viral levels by quantitative PCR. As shown in Fig. 5, there was no significant difference in PEDV attachment between control siRNA- and occludin siRNA-treated Vero E6 cells. Similar results were obtained

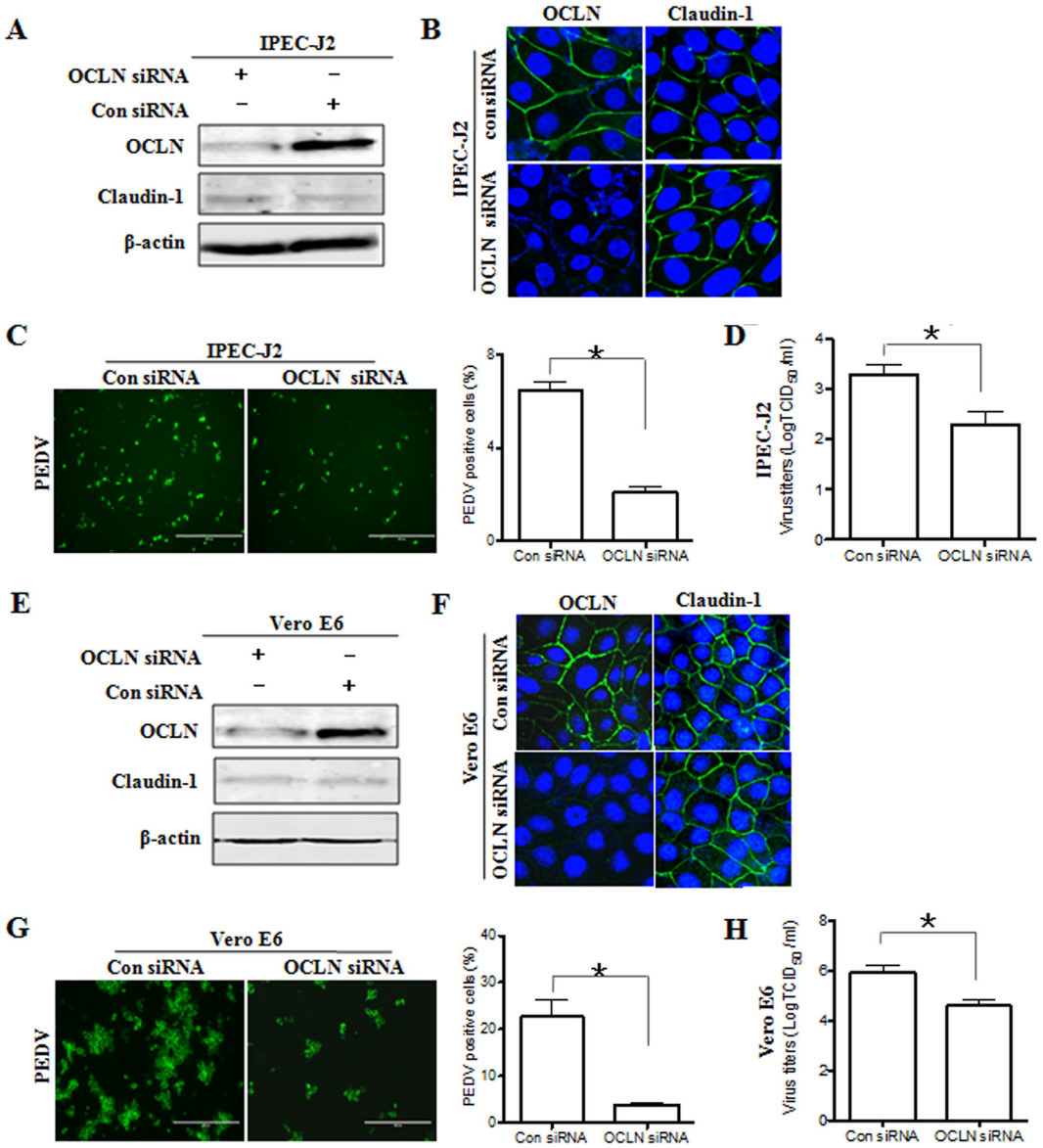

FIG 4 Depletion of endogenous occludin reduces viral infection. (A and E) Occludin knockdown efficiency was determined by Western blotting. Detergent lysates from IPEC-J2 (A) and Vero E6 (E) cells transfected with occludin-specific or scrambled control siRNA were subjected to immunoblotting with the indicated antibodies. (B and F) Occludin knockdown was confirmed by immunofluorescence assay. IPEC-J2 (B) and Vero E6 (F) cells were transfected with 100 nM siRNA duplexes against occludin or scrambled control siRNA. At 48 h posttransfection, cell monolayers were fixed and stained for occludin/claudin-1 (green) and the nucleus (blue). (C and G) Depletion of occludin suppresses PEDV infection. IPEC-J2 (C) and Vero E6 (G) cells were transfected with occludin-specific siRNA or control siRNA for 24 h, followed by infection with PEDV at MOIs of 1 and 0.1, respectively. At 24 hpi, the cell monolayers were fixed, and the numbers of PEDV-positive cells were determined by use of anti-PEDV spike protein MAb. (D and H) Occludin knockdown inhibits PEDV replication. IPEC-J2 (D) and Vero E6 (H) cells were exposed to PEDV 24 h after occludin-specific siRNA transfection. At 48 hpi, virus yields were determined by $TCID_{50}$ assay with Vero E6 cells. Results are representative of three independent experiments (means ± SD). *, $P < 0.05$. The P value was calculated using Student's t test.

with IPEC-J2 cells (Fig. 5). Western blot analysis showed that occludin siRNA reduced the endogenous occludin expression in both Vero E6 and IPEC-J2 cells (Fig. 4A and E). These data demonstrate that occludin is not involved in the initial attachment of virions to target cells, indicating that occludin acts at the postbinding stage of PEDV entry.

Inhibitors of macropinocytosis block both occludin internalization and PEDV entry. Previous data showed that binding of coronaviruses to target cells is followed by internalization of the viral particles via endocytosis (30). Macropinocytosis is a form of endocytosis which has been identified as an entry mechanism for several viral patho-

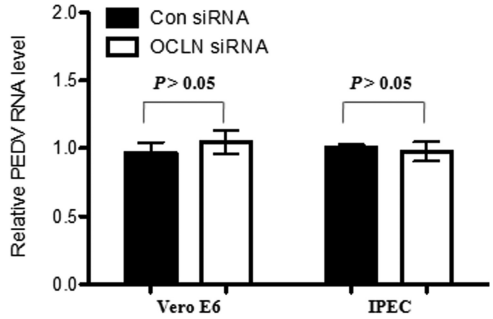

FIG 5 Occludin does not affect PEDV initial attachment. Vero E6 and IPEC-J2 cells were treated with occludin-specific or scrambled control siRNA for 24 h. After three washes with PBS, cells were incubated with PEDV at MOIs of 0.1 and 1 for Vero E6 and IPEC-J2 cells, respectively, for 2 h at 4°C. Unbound viral particles were removed by washing with ice-cold PBS five times. Total RNA was extracted, and the relative PEDV RNA level was analyzed by quantitative PCR as described in Materials and Methods. Data are presented as mean values ± SD (error bars) for three independent experiments performed in triplicate.

gens, including CBV, influenza virus, Ebola virus, vaccinia virus, HIV, and coronaviruses (31). As described above, we observed that PEDV infection induced the internalization of occludin, which might be due to its removal from the cell surface by macropinocytosis pathways (23). To determine whether macropinocytosis is involved in occludin and virus internalization, Vero E6 cells were pretreated with 5-(*N*-ethyl-*N*-isopropyl) amiloride (EIPA), which has largely been described as a macropinocytosis inhibitor (32). After treatment, the medium with EIPA was removed, and PEDV was added. The separation of EIPA treatment and virus incubation was done to ensure that the inhibitor was able to act only on host cells, not on the virus. We compared occludin and virus internalization levels in cells treated with a nontoxic dose of EIPA or with dimethyl sulfoxide (DMSO), the carrier control. As shown in Fig. 6A, EIPA prevented occludin and virus internalization. These data indicate that both occludin internalization and virus entry occur through a macropinocytotic pathway during PEDV infection. In these cells, EIPA pretreatment reduced the efficiency of PEDV infection (Fig. 6B) and decreased the viral yield (Fig. 6E). As was the case with Vero E6 cells, EIPA prevented occludin and virus internalization in PEDV-infected IPEC-J2 cells (Fig. 6C) and hampered virus infection (Fig. 6D) and subsequent replication (Fig. 6F). In addition, another macropinocytosis inhibitor, rottlerin (33), was used and showed similar patterns of inhibition of virus infection (Fig. 6E and F). Because we observed that the internalization of occludin through macropinocytosis is tightly associated with PEDV infection, the role of occludin in virus entry was further examined. We pretreated Vero E6 cells with EIPA to block the internalization of occludin (Fig. 6A) and then tested the virus distribution by using confocal microscopy. As shown in Fig. 7A, viral particles were randomly distributed in the perinuclear cytoplasm of DMSO-treated Vero E6 cells, while EIPA pretreatment trapped viral particles at the cellular junctional region and prevented them from entering the cytoplasm. However, only weak colocalization of occludin with PEDV protein was detected; thus, the occludin protein does not appear to interact directly with the virus. Similar results were obtained with IPEC-J2 cells (Fig. 7B). These findings reveal that inhibitors that block macropinocytosis block both occludin internalization and virus entry. It is worth mentioning that these results are similar to the reported macropinocytosis of CBV (23), suggesting that macropinocytosis-mediated occludin internalization is involved in PEDV entry.

To determine whether macropinocytosis is required for PEDV infection at a late stage, EIPA was added to the target cells after virus entry had occurred (4 hpi). Experiments showed that EIPA treatment did not block the internalization of occludin in virus-infected cells (data not shown). This macropinocytosis inhibitor did not inhibit PEDV entry and replication in either Vero E6 (Fig. 8A and B) or IPEC-J2 (Fig. 8C and D) cells. These data suggest that macropinocytosis or a macropinocytosis-like process is

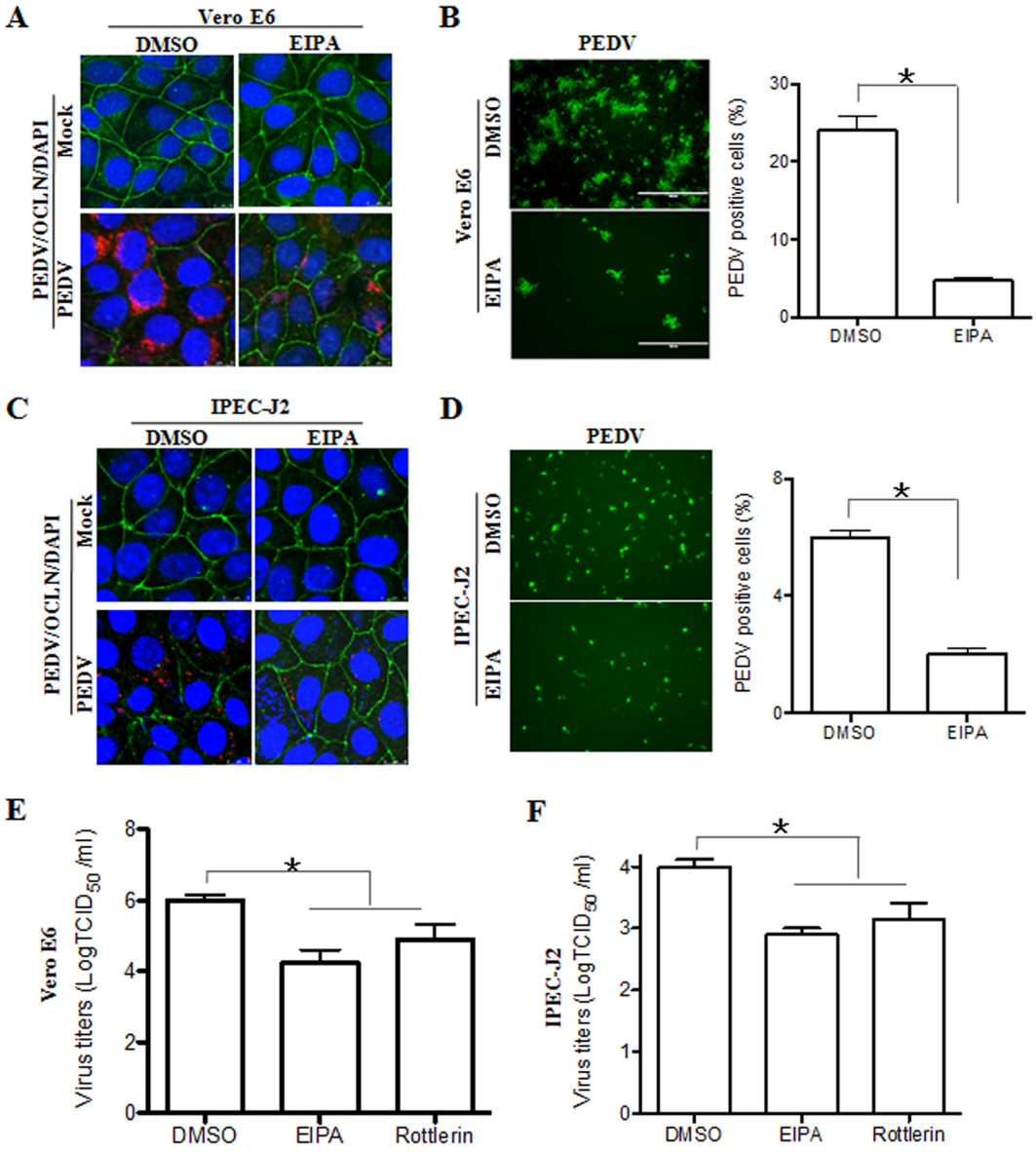

FIG 6 Macropinocytosis inhibitors block PEDV infection. (A and C) Occludin and virus internalization is blocked when cells are treated with EIPA. Vero E6 (A) and IPEC-J2 (C) cells were pretreated with the macropinocytosis inhibitor EIPA (50 μM) or the carrier control DMSO for 60 min. Cells were washed and infected with PEDV at MOIs of 0.1 and 1, respectively. At 12 hpi, cell monolayers were fixed and stained for PEDV (red), occludin (green), and the nucleus (blue). (B and D) Immunofluorescence assay to detect PEDV infection. Vero E6 and IPEC-J2 cells were treated with DMSO or EIPA for 1 h, followed by infection with PEDV at MOIs of 0.1 and 1, respectively. At 24 h postinoculation, cell monolayers were fixed, and the numbers of PEDV-positive cells were determined by immunofluorescence assay. (E and F) Macropinocytosis inhibitors reduce PEDV yields as determined by $TCID_{50}$ assay. Monolayers were exposed to PEDV for 1 h after treatment with DMSO, EIPA, or rottlerin (10 μM). At 48 hpi, virus yields were determined by a $TCID_{50}$ assay with Vero E6 cells. Data are shown as means $\pm$ SD for three separate experiments. *, $P < 0.05$. The P value was calculated using Student's t test.

involved in virus entry during early events of infection. Taken together, our data show that virus entry and the tight junction protein occludin seem to be closely coupled, suggesting that the occludin protein may serve as a scaffold in the vicinity of virus entry.

DISCUSSION

Tight junctions are composed of a group of highly specialized membrane proteins responsible for many important cellular functions. One of the key functions is to maintain adjacent cells close enough to each other to avoid the free passage of microorganisms across the paracellular space (34, 35). This tight junctional structure is

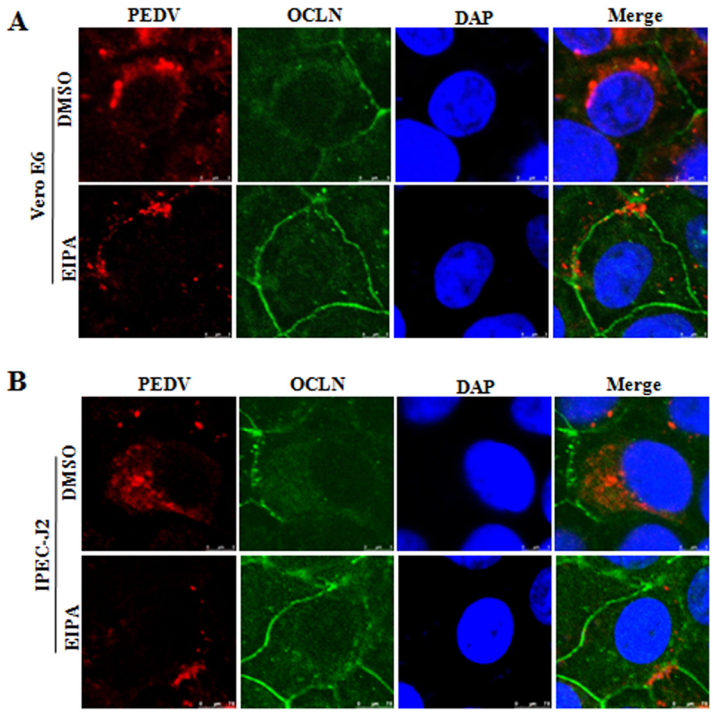

FIG 7 Macropinocytosis inhibitor inhibits PEDV entry. Vero E6 (A) and IPEC-J2 (B) cells were treated with EIPA for 1 h, followed by infection with PEDV at MOIs of 0.1 and 1, respectively, for a further 4 h. Cell monolayers were fixed, and triple-color immunofluorescence staining was performed to detect the PEDV spike protein (red), occludin (green), and the nucleus (blue). Images are representative of three independent experiments.

widely distributed in epithelial cells as a primary physical barrier, especially in the intestinal epithelium. Emerging evidence indicates that tight junctions are not an absolute barrier but rather an important component in the infection of several viruses (21). In this study, we found that internalization of the tight junction protein occludin occurs by a macropinocytosis-like process upon PEDV infection. Inhibitors that block macropinocytosis can block both occludin internalization and virus entry. These data along with the fact that occludin knockdown impairs PEDV infection strongly suggest that occludin plays an essential role in the PEDV entry process.

To infect its host, a virus must first enter target cells at the body surface. The most common route of viral entry is to break epithelial cell barriers to establish infection. Tight junctions correlate with the maintenance of the paracellular barrier function in epithelial cells even when epithelial cells divide (36, 37). In the experiments reported here, we demonstrated, for the first time, that PEDV induces occludin internalization in virus-infected cells, indicating an alteration in the barrier properties of the epithelium. In addition, the relocalization of occludin upon PEDV infection is also seen in noninfected cells, suggesting indirect effects of PEDV on the cellular distribution of occludin. Since others have reported that PEDV-infected Vero E6 and IPEC-J2 cells do not produce type I interferon (38, 39), we infer that the internalization of occludin in noninfected cells may be induced by some other pathophysiologic stimuli, such as proinflammatory cytokines (40). Jung and colleagues demonstrated that PEDV infection resulted in structurally altered tight junction proteins ZO-1 and E-cadherin in the villous epithelium *in vivo* (41). Other viruses that are capable of causing diarrhea, such as rotaviruses, infect intestinal columnar epithelial cells and significantly alter the distribution of the tight junction proteins claudin-1 and occludin to promote virus infection (42). A similar event has been observed during human CBV infection, which alters the integrity of tight junctions and induces occludin internalization (23). Surprisingly, we observed that PEDV upregulates the expression level of the occludin protein. In most cases, host cells that were infected with pathogens showed decreased expression of tight junction

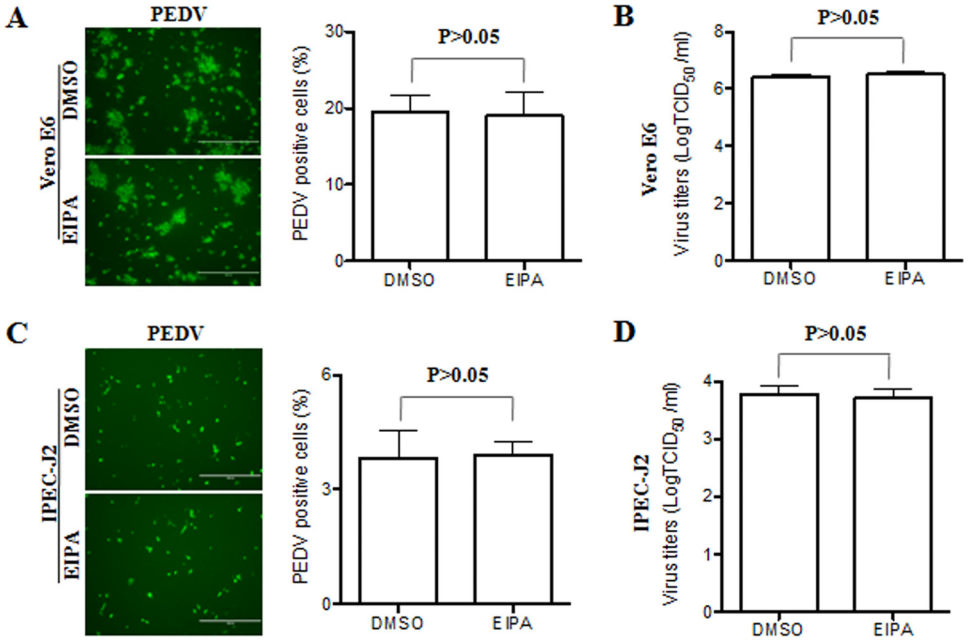

FIG 8 Macropinocytosis inhibitor does not affect virus infection at a late stage. (A and C) PEDV infection was determined by immunofluorescence assay. Vero E6 (A) and IPEC-J2 (C) cells were infected with PEDV for 4 h and then incubated in medium containing DMSO or EIPA. Twenty-four hours after inoculation, the cell monolayers were fixed and examined for PEDV infection by immunofluorescence assay with FITC-conjugated PEDV spike protein MAb. The PEDV-positive cells were counted in three independent experiments, and values shown are means ± SD. *, $P < 0.05$. The P value was calculated using Student's t test. (B and D) Virus yields were determined by $TCID_{50}$ assay. Monolayers were first inoculated with PEDV and then incubated in medium containing DMSO or EIPA. At 48 hpi, virus yields were determined by a $TCID_{50}$ assay with Vero E6 cells. All values are representative of three independent experiments.

proteins, such as claudin-1 and occludin (43–46). Although it is not clear why PEDV induces the upregulation of occludin, there are two likely possibilities. The first is that the maintenance of the epithelial barrier is associated with restoration of tight junction structures and increased expression of tight junction proteins (47, 48). The second possibility is that the inflammatory mediators secreted by virus-infected cells play important roles in the modification of tight junction protein expression (25, 49, 50).

Currently, it seems that PEDV infection is initiated by binding of the viral spike protein to the cellular receptor porcine APN, followed by the entry process (17, 18, 51). Contradictory results have been reported concerning the PEDV functional receptor. Shirato et al. reported that porcine APN is not a cellular receptor of PEDV (52), suggesting that some other cellular factor(s) might be involved in infection by PEDV. Here we show that overexpression of occludin facilitates PEDV infection and that knockdown of occludin expression inhibits virus infection in PEDV-susceptible cell lines. However, upon overexpression of occludin, a PEDV-resistant cell line remained unsusceptible to PEDV. These data suggest that the tight junction protein occludin contributes to PEDV infection and acts as an entry cofactor. Similarly, CBV can use the tight junction protein occludin as a coreceptor to infect polarized epithelium (23). Additionally, human occludin is an HCV entry factor required for infection of mouse cells (24).

Numerous viruses have been found to use proteins of more than one molecular species as receptors for cell infection. Distinct receptor interactions may be required for specific events in the process of virus infection, such that one receptor may permit virus to attach to the cell surface and a second may facilitate virus entry into the cytoplasm (53). Our data show that the occludin protein does not mediate the initial attachment of virions to target cells, suggesting that occludin appears not to interact directly with virus at the cell surface. These findings indicate that another attachment receptor(s), such as cell surface heparan sulfate (54), may serve to bind the viral particles and thus help to concentrate viruses on the cell surface.

It has been known that coronavirus entry into cells occurs via direct fusion at the

TABLE 1 PCR primers used for this study

Primer	Sequence (5′–3′)
occludin-F[a]	CCG**CTCGAG**ATGTCATCCAGGCCTCTTGAA
occludin-R[a]	ATTT*GCGGCCGC*CTACTTGTCGTCATCGTCTTTGTAGTCTGTTTTCCTTCGATCATAAT
PEDV-F[b]	GCACTTATTGGCAGGCTTTGT
PEDV-R[b]	CCATTGAGAAAAGAAAGTGTCGTAG
occludin-F[b]	ACGAGCTGGAGGAAGACTGGATC
occludin-R[b]	GATCCCTTAACTTGCTTCAGTCTATTG
claudin-1-F[b]	CCTACGCTGGTGACAACATTG
claudin-1-R[b]	CACTTCATGCCAACAGTGGC
Monkey β-actin-F[b]	AGGCTCTCTTCCAACCTTCCTT
Monkey β-actin-R[b]	CGTACAGGTCTTTACGGATGTCCA
Porcine β-actin-F[b]	CTTCCTGGGCATGGAGTCC
Porcine β-actin-R[b]	GGCGCGATGATCTTGATCTTC

[a]A Flag tag (underlined) was fused at the carboxyl terminus of occludin by PCR and was cloned into the XhoI (bold) and NotI (italics) sites in the pLVX-IRES-ZsGreen1 vector.
[b]Used for relative quantitative PCR.

plasma membrane or by endocytosis (51). Previous research reported that occludin not only is a key player in transepithelial barrier function but also may be involved in the biogenesis of endocytic vesicles (55). In this study, we found that EIPA, a hallmark inhibitor of macropinocytosis, inhibited occludin internalization and PEDV entry. Immunofluorescence microscopy data provide solid evidence that EIPA traps viral particles at the junctional regions of virus-infected cells. Our findings suggest that macropinocytosis of virus is coupled to the internalization of occludin. Macropinocytosis has emerged as a major form of endocytosis in which small particles are brought into cells. Many viruses, such as HIV and influenza A virus, employ macropinocytosis to gain entry into host cells (31, 56, 57). However, once viral entry has occurred, EIPA cannot block PEDV infection, suggesting that macropinocytosis- or macropinocytosis-like process-mediated virus entry is an early event in virus infection. Moreover, although we demonstrated that the tight junction protein occludin is an important PEDV entry factor, significant colocalization of occludin with PEDV protein was not evident, which suggests that occludin may serve as a scaffold in the vicinity of virus entry.

Based on these results, we conclude that although occludin does not directly bind PEDV on the cell surface and is not associated with PEDV in the cytoplasm, it is nonetheless essential for early steps of virus entry. Although the detailed interplay between occludin and PEDV remains incompletely understood, it is possible that occludin facilitates virus internalization by recruiting some other regulatory molecules. Further work is needed to conclusively answer this question. Together, these findings provide novel insights into PEDV infection and spreading, which might be valuable for understanding PEDV-related pathogenesis.

MATERIALS AND METHODS

Cells and viruses. Vero E6 (African green monkey kidney epithelial cells), IPEC-J2 (porcine intestinal epithelial cell clone J2), and BHK (baby hamster kidney fibroblasts) cell lines were grown and maintained in Dulbecco minimum essential medium (DMEM) supplemented with 10% heat-inactivated fetal bovine serum (FBS; Thermo Fisher) (58). All cells were cultured in a humidified atmosphere at 37°C and 5% CO_2. PEDV strain CV777 (GenBank accession number KT323979) was grown and titrated in Vero E6 cells.

Overexpression of occludin in Vero E6 and IPEC-J2 cells. The occludin gene was amplified from porcine intestinal epithelium cDNA by use of the primers listed in Table 1 and then cloned into the bicistronic lentivirus vector pLVX-IRES-ZsGreen1 (Clontech). The nucleotide sequences of the plasmids expressing occludin were determined to ensure that the correct clones were used in this study. The packaging and production of lentiviral vectors were performed as previously described (59). When Vero E6 and IPEC-J2 cells reached 80% confluence, cell monolayers were transduced with recombinant lentivirus at a multiplicity of infection (MOI) of 20 with 4 μg/ml Polybrene (Sigma). At 24 h postincubation, the cells and supernatants were harvested for further analysis.

RNA interference. Small interfering RNA (siRNA) duplexes were introduced to knock down endogenous occludin expression. Vero E6 and IPEC-J2 cells were transfected with 100 nM occludin-specific or scrambled control siRNA duplexes (Table 2) by use of Lipofectamine RNAiMAX reagent (Invitrogen) according to the manufacturer's instructions. Twenty-four hours after transfection, cells were prepared

TABLE 2 Sequences of siRNA sense strands used to ablate occludin protein expression in Vero E6 or IPEC-J2 cells

Double-stranded RNA	Sense strand sequence (5′-3′)	Target
siRNA 1	UUGUAAGCUCUUGUACUCCTT	Monkey occludin
siRNA 2	UAAGCUCUUGUACUCCUGCTT	Porcine occludin
Control siRNA	UUCUCCGAACGUGUCAGCUTT	Scrambled sequence

and assayed for specific gene silencing by immunofluorescence microscopy and Western blotting. In some experiments, at 24 h posttransfection, PEDV infection was performed at MOIs of 0.1 and 1 for Vero E6 and IPEC-J2 cells, respectively.

Pharmacological inhibitors. The macropinocytosis inhibitors 5-(*N*-ethyl-*N*-isopropyl) amiloride (EIPA) and rottlerin (60, 61) (Sigma) were used at 50 μM and 10 μM, respectively. Vero E6 and IPEC-J2 cells were pretreated with inhibitors or the carrier control DMSO for 1 h at 37°C. After removal of the drugs, cell monolayers were infected with PEDV at MOIs of 0.1 and 1 for Vero E6 and IPEC-J2 cells, respectively. At 4 or 12 hpi, the cells were fixed for subsequent determination of the occludin distribution and virus infection. In some experiments, cells were first infected with PEDV for 4 h and then incubated with the drugs as described above to assess the effects of drugs on virus replication.

Virus binding assay. At 24 h post-siRNA transfection, Vero E6 and IPEC-J2 cells were washed with ice-cold phosphate-buffered saline (PBS) and then incubated with PEDV for 2 h at 4°C, at MOIs of 0.1 and 1, respectively. The exposed cells were then washed five times with ice-cold PBS to remove excess virions. Viral RNA was quantified by quantitative PCR.

Quantitative PCR. RNA extraction, reverse transcription (RT), and quantitative PCR were performed as previously described (62). In brief, relative quantification was performed by the cycle threshold ($\Delta\Delta C_T$) method (63). All the gene-specific primers are listed in Table 1.

Confocal immunofluorescence microscopy. Confocal microscopy was performed as described previously (64), with slight modifications. After various treatments, the Vero E6 and IPEC-J2 cell monolayers were washed twice with PBS and fixed in methanol for 20 min at −20°C. After blocking, cells were incubated with rabbit anti-occludin polyclonal antibody (Thermo Fisher) or rabbit anti-claudin-1 monoclonal antibody (MAb) (Santa Cruz Biotechnology). After washing, cells were incubated with fluorescein isothiocyanate (FITC)/tetramethyl rhodamine isocyanate (TRITC)-conjugated goat anti-rabbit or anti-mouse IgG (Jackson ImmunoResearch). For some experiments, cells were incubated with mouse anti-PEDV spike protein MAb (Median Diagnostics, South Korea) followed by incubation with FITC/TRITC-conjugated goat anti-mouse IgG (Jackson ImmunoResearch). Lastly, cells were stained with DAPI (4′,6-diamidino-2-phenylindole) for 5 min and then examined with a Leica SP2 laser scanning spectrum confocal system (Leica Microsystems).

Immunofluorescence assay. An immunofluorescence assay was performed as previously described (58). Briefly, Vero E6 and IPEC-J2 cell monolayers were inoculated with PEDV at MOIs of 0.1 and 1, respectively. At 24 hpi, cells were fixed, stained with mouse anti-PEDV spike protein MAb (Median Diagnostics, South Korea), and then incubated with FITC/TRITC-conjugated goat anti-mouse IgG (Jackson ImmunoResearch). Fluorescence was visualized with an Olympus inverted fluorescence microscope equipped with a camera.

Western blot assay. Western blot analysis was done as described previously (65), with slight modifications. Typically, samples were separated by SDS-PAGE under reducing conditions and transferred to a polyvinylidene difluoride (PVDF) membrane. After blocking, the membranes were incubated with a primary antibody and then incubated with an IRDye-conjugated secondary antibody (Li-Cor). The rabbit anti-occludin polyclonal antibody was purchased from Abcam. The rabbit anti-claudin-1 MAb and mouse anti-β-actin MAb were purchased from Santa Cruz Biotechnology. The mouse anti-PEDV nucleocapsid protein MAb was prepared in our laboratory.

Statistical analysis. Values are expressed as means ± standard deviations (SD). Data were analyzed using Student's *t* test and analyzed using Prism 5. *P* values of <0.05 were considered significant.

Accession number(s). The nucleotide sequences of the plasmids encoding occludin were deposited in GenBank under accession number NM_001163647.2.

ACKNOWLEDGMENTS

This research was supported by grants from the National Natural Science Foundation of China (grant 31572497) and the Natural Science Foundation of Heilongjiang Province (grant JC2016005).

REFERENCES

1. Fehr AR, Perlman S. 2015. Coronaviruses: an overview of their replication and pathogenesis. Methods Mol Biol 1282:1–23. https://doi.org/10.1007/978-1-4939-2438-7_1.
2. Fehr AR, Athmer J, Channappanavar R, Phillips JM, Meyerholz DK, Perlman S. 2015. The nsp3 macrodomain promotes virulence in mice with coronavirus-induced encephalitis. J Virol 89:1523–1536. https://doi.org/10.1128/JVI.02596-14.
3. Song D, Park B. 2012. Porcine epidemic diarrhoea virus: a comprehensive review of molecular epidemiology, diagnosis, and vaccines. Virus Genes 44:167–175. https://doi.org/10.1007/s11262-012-0713-1.

4. Kocherhans R, Bridgen A, Ackermann M, Tobler K. 2001. Completion of the porcine epidemic diarrhoea coronavirus (PEDV) genome sequence. Virus Genes 23:137–144. https://doi.org/10.1023/A:1011831902219.
5. Chen J, Liu X, Lang H, Wang Z, Shi D, Shi H, Zhang X, Feng L. 2013. Genetic variation of nucleocapsid genes of porcine epidemic diarrhea virus field strains in China. Arch Virol 158:1397–1401. https://doi.org/10.1007/s00705-013-1608-8.
6. Chen Q, Li G, Stasko J, Thomas JT, Stensland WR, Pillatzki AE, Gauger PC, Schwartz KJ, Madson D, Yoon KJ, Stevenson GW, Burrough ER, Harmon KM, Main RG, Zhang J. 2014. Isolation and characterization of porcine epidemic diarrhea viruses associated with the 2013 disease outbreak among swine in the United States. J Clin Microbiol 52:234–243. https://doi.org/10.1128/JCM.02820-13.
7. Ducatelle R, Coussement W, Pensaert MB, Debouck P, Hoorens J. 1981. In vivo morphogenesis of a new porcine enteric coronavirus, CV 777. Arch Virol 68:35–44. https://doi.org/10.1007/BF01315165.
8. Huang YW, Dickerman AW, Pineyro P, Li L, Fang L, Kiehne R, Opriessnig T, Meng XJ. 2013. Origin, evolution, and genotyping of emergent porcine epidemic diarrhea virus strains in the United States. mBio 4:e00737-13. https://doi.org/10.1128/mBio.00737-13.
9. Kim YK, Lim SI, Lim JA, Cho IS, Park EH, Le VP, Hien NB, Thach PN, Quynh D, Vui HTQ, Tien NT, An DJ. 2015. A novel strain of porcine epidemic diarrhea virus in Vietnamese pigs. Arch Virol 160:1573–1577. https://doi.org/10.1007/s00705-015-2411-5.
10. Pensaert MB, de Bouck P. 1978. A new coronavirus-like particle associated with diarrhea in swine. Arch Virol 58:243–247. https://doi.org/10.1007/BF01317606.
11. Lee HM, Lee BJ, Tae JH, Kweon CH, Lee YS, Park JH. 2000. Detection of porcine epidemic diarrhea virus by immunohistochemistry with recombinant antibody produced in phages. J Vet Med Sci 62:333–337. https://doi.org/10.1292/jvms.62.333.
12. Jung K, Wang Q, Scheuer KA, Lu Z, Zhang Y, Saif LJ. 2014. Pathology of US porcine epidemic diarrhea virus strain PC21A in gnotobiotic pigs. Emerg Infect Dis 20:662–665. https://doi.org/10.3201/eid2004.131685.
13. Tsukita S, Furuse M, Itoh M. 2001. Multifunctional strands in tight junctions. Nat Rev Mol Cell Biol 2:285–293. https://doi.org/10.1038/35067088.
14. Anderson JM, Van Itallie CM. 1999. Tight junctions: closing in on the seal. Curr Biol 9:R922–R924. https://doi.org/10.1016/S0960-9822(00)80105-0.
15. Aijaz S, Balda MS, Matter K. 2006. Tight junctions: molecular architecture and function. Int Rev Cytol 248:261–298. https://doi.org/10.1016/S0074-7696(06)48005-0.
16. Li BX, Ge JW, Li YJ. 2007. Porcine aminopeptidase N is a functional receptor for the PEDV coronavirus. Virology 365:166–172. https://doi.org/10.1016/j.virol.2007.03.031.
17. Oh JS, Song DS, Park BK. 2003. Identification of a putative cellular receptor 150 kDa polypeptide for porcine epidemic diarrhea virus in porcine enterocytes. J Vet Sci 4:269–275.
18. Park JE, Park ES, Yu JE, Rho J, Paudel S, Hyun BH, Yang DK, Shin HJ. 2015. Development of transgenic mouse model expressing porcine aminopeptidase N and its susceptibility to porcine epidemic diarrhea virus. Virus Res 197:108–115. https://doi.org/10.1016/j.virusres.2014.12.024.
19. Grove J, Marsh M. 2011. The cell biology of receptor-mediated virus entry. J Cell Biol 195:1071–1082. https://doi.org/10.1083/jcb.201108131.
20. Guttman JA, Finlay BB. 2009. Tight junctions as targets of infectious agents. Biochim Biophys Acta 1788:832–841. https://doi.org/10.1016/j.bbamem.2008.10.028.
21. Torres-Flores JM, Arias CF. 2015. Tight junctions go viral! Viruses 7:5145–5154. https://doi.org/10.3390/v7092865.
22. Zeisel MB, Turek M, Baumert TF. 2010. Getting closer to the patient: upgrade of hepatitis C virus infection in primary human hepatocytes. J Hepatol 53:388–389. https://doi.org/10.1016/j.jhep.2010.04.004.
23. Coyne CB, Shen L, Turner JR, Bergelson JM. 2007. Coxsackievirus entry across epithelial tight junctions requires occludin and the small GTPases Rab34 and Rab5. Cell Host Microbe 2:181–192. https://doi.org/10.1016/j.chom.2007.07.003.
24. Ploss A, Evans MJ, Gaysinskaya VA, Panis M, You H, de Jong YP, Rice CM. 2009. Human occludin is a hepatitis C virus entry factor required for infection of mouse cells. Nature 457:882–886. https://doi.org/10.1038/nature07684.
25. Roe K, Kumar M, Lum S, Orillo B, Nerurkar VR, Verma S. 2012. West Nile virus-induced disruption of the blood-brain barrier in mice is characterized by the degradation of the junctional complex proteins and increase in multiple matrix metalloproteinases. J Gen Virol 93:1193–1203. https://doi.org/10.1099/vir.0.040899-0.
26. Benedicto I, Molina-Jimenez F, Barreiro O, Maldonado-Rodriguez A, Prieto J, Moreno-Otero R, Aldabe R, Lopez-Cabrera M, Majano PL. 2008. Hepatitis C virus envelope components alter localization of hepatocyte tight junction-associated proteins and promote occludin retention in the endoplasmic reticulum. Hepatology 48:1044–1053. https://doi.org/10.1002/hep.22465.
27. Che P, Tang H, Li Q. 2013. The interaction between claudin-1 and dengue viral prM/M protein for its entry. Virology 446:303–313. https://doi.org/10.1016/j.virol.2013.08.009.
28. Evans MJ, von Hahn T, Tscherne DM, Syder AJ, Panis M, Wolk B, Hatzioannou T, McKeating JA, Bieniasz PD, Rice CM. 2007. Claudin-1 is a hepatitis C virus co-receptor required for a late step in entry. Nature 446:801–805. https://doi.org/10.1038/nature05654.
29. Zhao S, Gao J, Zhu L, Yang Q. 2014. Transmissible gastroenteritis virus and porcine epidemic diarrhoea virus infection induces dramatic changes in the tight junctions and microfilaments of polarized IPEC-J2 cells. Virus Res 192:34–45. https://doi.org/10.1016/j.virusres.2014.08.014.
30. Burkard C, Verheije MH, Wicht O, van Kasteren SI, van Kuppeveld FJ, Haagmans BL, Pelkmans L, Rottier PJ, Bosch BJ, de Haan CA. 2014. Coronavirus cell entry occurs through the endo-/lysosomal pathway in a proteolysis-dependent manner. PLoS Pathog 10:e1004502. https://doi.org/10.1371/journal.ppat.1004502.
31. Mercer J, Helenius A. 2009. Virus entry by macropinocytosis. Nat Cell Biol 11:510–520. https://doi.org/10.1038/ncb0509-510.
32. Koivusalo M, Welch C, Hayashi H, Scott CC, Kim M, Alexander T, Touret N, Hahn KM, Grinstein S. 2010. Amiloride inhibits macropinocytosis by lowering submembranous pH and preventing Rac1 and Cdc42 signaling. J Cell Biol 188:547–563. https://doi.org/10.1083/jcb.200908086.
33. Sakharkar AJ, Singru PS, Sarkar K, Subhedar NK. 2005. Neuropeptide Y in the forebrain of the adult male cichlid fish Oreochromis mossambicus: distribution, effects of castration and testosterone replacement. J Comp Neurol 489:148–165. https://doi.org/10.1002/cne.20614.
34. Shen L. 2012. Tight junctions on the move: molecular mechanisms for epithelial barrier regulation. Ann N Y Acad Sci 1258:9–18. https://doi.org/10.1111/j.1749-6632.2012.06613.x.
35. Steed E, Balda MS, Matter K. 2010. Dynamics and functions of tight junctions. Trends Cell Biol 20:142–149. https://doi.org/10.1016/j.tcb.2009.12.002.
36. Jinguji Y, Ishikawa H. 1992. Electron microscopic observations on the maintenance of the tight junction during cell division in the epithelium of the mouse small intestine. Cell Struct Funct 17:27–37. https://doi.org/10.1247/csf.17.27.
37. Saladik DT, Soler AP, Lewis SA, Mullin JM. 1995. Cell division does not increase transepithelial permeability of LLC-PK1 cell sheets. Exp Cell Res 220:446–455. https://doi.org/10.1006/excr.1995.1336.
38. Cao L, Ge X, Gao Y, Zarlenga DS, Wang K, Li X, Qin Z, Yin X, Liu J, Ren X, Li G. 2015. Putative phage-display epitopes of the porcine epidemic diarrhea virus S1 protein and their anti-viral activity. Virus Genes 51:217–224. https://doi.org/10.1007/s11262-015-1234-5.
39. Xing Y, Chen J, Tu J, Zhang B, Chen X, Shi H, Baker SC, Feng L, Chen Z. 2013. The papain-like protease of porcine epidemic diarrhea virus negatively regulates type I interferon pathway by acting as a viral deubiquitinase. J Gen Virol 94:1554–1567. https://doi.org/10.1099/vir.0.051169-0.
40. Han X, Fink MP, Delude RL. 2003. Proinflammatory cytokines cause NO*-dependent and -independent changes in expression and localization of tight junction proteins in intestinal epithelial cells. Shock 19:229–237. https://doi.org/10.1097/00024382-200303000-00006.
41. Jung K, Eyerly B, Annamalai T, Lu Z, Saif LJ. 2015. Structural alteration of tight and adherens junctions in villous and crypt epithelium of the small and large intestine of conventional nursing piglets infected with porcine epidemic diarrhea virus. Vet Microbiol 177:373–378. https://doi.org/10.1016/j.vetmic.2015.03.022.
42. Dickman KG, Hempson SJ, Anderson J, Lippe S, Zhao L, Burakoff R, Shaw RD. 2000. Rotavirus alters paracellular permeability and energy metabolism in Caco-2 cells. Am J Physiol Gastrointest Liver Physiol 279:G757–G766.
43. Burgel N, Bojarski C, Mankertz J, Zeitz M, Fromm M, Schulzke JD. 2002. Mechanisms of diarrhea in collagenous colitis. Gastroenterology 123:433–443. https://doi.org/10.1053/gast.2002.34784.
44. Huber JD, Witt KA, Hom S, Egleton RD, Mark KS, Davis TP. 2001. Inflammatory pain alters blood-brain barrier permeability and tight junctional protein expression. Am J Physiol Heart Circ Physiol 280:H1241–H1248.

45. McDermott JR, Bartram RE, Knight PA, Miller HR, Garrod DR, Grencis RK. 2003. Mast cells disrupt epithelial barrier function during enteric nematode infection. Proc Natl Acad Sci U S A 100:7761–7766. https://doi.org/10.1073/pnas.1231488100.
46. Yoshida Y, Morita K, Mizoguchi A, Ide C, Miyachi Y. 2001. Altered expression of occludin and tight junction formation in psoriasis. Arch Dermatol Res 293:239–244. https://doi.org/10.1007/s004030100221.
47. Miyauchi E, Morita H, Tanabe S. 2009. Lactobacillus rhamnosus alleviates intestinal barrier dysfunction in part by increasing expression of zonula occludens-1 and myosin light-chain kinase in vivo. J Dairy Sci 92:2400–2408. https://doi.org/10.3168/jds.2008-1698.
48. Ukena SN, Singh A, Dringenberg U, Engelhardt R, Seidler U, Hansen W, Bleich A, Bruder D, Franzke A, Rogler G, Suerbaum S, Buer J, Gunzer F, Westendorf AM. 2007. Probiotic Escherichia coli Nissle 1917 inhibits leaky gut by enhancing mucosal integrity. PLoS One 2:e1308. https://doi.org/10.1371/journal.pone.0001308.
49. Abdulnour-Nakhoul SM, Al-Tawil Y, Gyftopoulos AA, Brown KL, Hansen M, Butcher KF, Eidelwein AP, Noel RA, Rabon E, Posta A, Nakhoul NL. 2013. Alterations in junctional proteins, inflammatory mediators and extracellular matrix molecules in eosinophilic esophagitis. Clin Immunol 148:265–278. https://doi.org/10.1016/j.clim.2013.05.004.
50. Lechner J, Krall M, Netzer A, Radmayr C, Ryan MP, Pfaller W. 1999. Effects of interferon alpha-2b on barrier function and junctional complexes of renal proximal tubular LLC-PK1 cells. Kidney Int 55:2178–2191. https://doi.org/10.1046/j.1523-1755.1999.00487.x.
51. Belouzard S, Millet JK, Licitra BN, Whittaker GR. 2012. Mechanisms of coronavirus cell entry mediated by the viral spike protein. Viruses 4:1011–1033. https://doi.org/10.3390/v4061011.
52. Shirato K, Maejima M, Islam MT, Miyazaki A, Kawase M, Matsuyama S, Taguchi F. 2016. Porcine aminopeptidase N is not a cellular receptor of porcine epidemic diarrhea virus, but promotes its infectivity via aminopeptidase activity. J Gen Virol 97:2528–2539. https://doi.org/10.1099/jgv.0.000563.
53. Marsh M, Helenius A. 2006. Virus entry: open sesame. Cell 124:729–740. https://doi.org/10.1016/j.cell.2006.02.007.
54. Huan CC, Wang Y, Ni B, Wang R, Huang L, Ren XF, Tong GZ, Ding C, Fan HJ, Mao X. 2015. Porcine epidemic diarrhea virus uses cell-surface heparan sulfate as an attachment factor. Arch Virol 160:1621–1628. https://doi.org/10.1007/s00705-015-2408-0.
55. Feldman GJ, Mullin JM, Ryan MP. 2005. Occludin: structure, function and regulation. Adv Drug Deliv Rev 57:883–917. https://doi.org/10.1016/j.addr.2005.01.009.
56. de Vries E, Tscherne DM, Wienholts MJ, Cobos-Jimenez V, Scholte F, Garcia-Sastre A, Rottier PJ, de Haan CA. 2011. Dissection of the influenza A virus endocytic routes reveals macropinocytosis as an alternative entry pathway. PLoS Pathog 7:e1001329. https://doi.org/10.1371/journal.ppat.1001329.
57. Mercer J, Helenius A. 2012. Gulping rather than sipping: macropinocytosis as a way of virus entry. Curr Opin Microbiol 15:490–499. https://doi.org/10.1016/j.mib.2012.05.016.
58. Guo L, Luo X, Li R, Xu Y, Zhang J, Ge J, Bu Z, Feng L, Wang Y. 2016. Porcine epidemic diarrhea virus infection inhibits interferon signaling by targeted degradation of STAT1. J Virol 90:8281–8292. https://doi.org/10.1128/JVI.01091-16.
59. Li R, Guo L, Gu W, Luo X, Zhang J, Xu Y, Tian Z, Feng L, Wang Y. 2016. Production of porcine TNFalpha by ADAM17-mediated cleavage negatively regulates porcine reproductive and respiratory syndrome virus infection. Immunol Res 64:711–720. https://doi.org/10.1007/s12026-015-8772-8.
60. Sarkar K, Kruhlak MJ, Erlandsen SL, Shaw S. 2005. Selective inhibition by rottlerin of macropinocytosis in monocyte-derived dendritic cells. Immunology 116:513–524.
61. Meier O, Boucke K, Hammer SV, Keller S, Stidwill RP, Hemmi S, Greber UF. 2002. Adenovirus triggers macropinocytosis and endosomal leakage together with its clathrin-mediated uptake. J Cell Biol 158:1119–1131. https://doi.org/10.1083/jcb.200112067.
62. Guo L, Niu J, Yu H, Gu W, Li R, Luo X, Huang M, Tian Z, Feng L, Wang Y. 2014. Modulation of CD163 expression by metalloprotease ADAM17 regulates porcine reproductive and respiratory syndrome virus entry. J Virol 88:10448–10458. https://doi.org/10.1128/JVI.01117-14.
63. Livak KJ, Schmittgen TD. 2001. Analysis of relative gene expression data using real-time quantitative PCR and the 2(−Delta Delta C(T)) method. Methods 25:402–408. https://doi.org/10.1006/meth.2001.1262.
64. Gu W, Guo L, Yu H, Niu J, Huang M, Luo X, Li R, Tian Z, Feng L, Wang Y. 2015. Involvement of CD16 in antibody-dependent enhancement of porcine reproductive and respiratory syndrome virus infection. J Gen Virol 96:1712–1722. https://doi.org/10.1099/vir.0.000118.
65. Guo L, Yu H, Gu W, Luo X, Li R, Zhang J, Xu Y, Yang L, Shen N, Feng L, Wang Y. 2016. Autophagy negatively regulates transmissible gastroenteritis virus replication. Sci Rep 6:23864. https://doi.org/10.1038/srep23864.